ABSTRACT: Recent work implicates excitotoxicity-induced apoptosis as the mechanism triggering motor neuron death in amyotrophic lateral sclerosis (ALS). Our laboratory has previously utilized glutamate excitotoxicity in vitro to study this process. The present experiment tests whether overexpression of the gene for Bcl-$_x$L can inhibit excitotoxicity in this model system. To track Bcl-$_x$L expression, the gene for green fluorescent protein (GFP) was inserted in-frame, upstream of the Bcl-$_x$L gene. The GFP-Bcl-$_x$L gene was then cloned into an adeno-associated viral (AAV2) vector. GFP expression in both SH-SY5Y and embryonic day 15 (E15) motor neurons (MNs) peaked 48 hours after infection. Bcl-$_x$L expression in SH-SY5Y cells significantly reduced terminal deoxy-UTP nick-end labeling (TUNEL)–positive cells and maintained cell density after glutamate exposure. Similarly, Bcl-$_x$L expression inhibited the development of TUNEL staining in E15 MNs and supported cell density after glutamate exposure. These findings suggest that AAV-mediated expression of genes for antiapoptotic proteins may provide a means for ALS gene therapy.

Muscle Nerve **32:** 734–744, 2005

NEUROPROTECTIVE ADENO-ASSOCIATED VIRUS Bcl-$_x$L GENE TRANSFER IN MODELS OF MOTOR NEURON DISEASE

MARY E. GARRITY-MOSES, BS, QINGSHAN TENG, MD, MSc, JAMES LIU, BS, DIANA TANASE, MD, PhD, and NICHOLAS M. BOULIS, MD

Departments of Neurological Surgery and Neurosciences, Lerner Research Institute, Cleveland Clinic Foundation, NB 2 120, 9500 Euclid Avenue, Cleveland, Ohio 44195, USA

Accepted 27 June 2005

Amyotrophic lateral sclerosis (ALS) is a neurodegenerative disease characterized by the death of spinal and cortical motor neurons. The loss of motor neurons (MNs) causes weakness that usually becomes symptomatic in the sixth decade of life, with a mean survival of 4 years from onset.[38] Currently, the only available treatment, riluzole, increases survival by a matter of months. Otherwise, treatment is largely palliative.[5] Approximately 2% of human ALS is associated with a dominantly inherited mutation of the Cu/Zn superoxide dismutase gene (*SOD1*).[35] Transgenic mice overexpressing mutant *SOD1* have provided a useful means of exploring the etiology of ALS.[21,48]

Recent data suggest that viral gene transfer may provide a means to treat ALS. Our laboratory[6] and others have recently observed that peripheral nerve injection and intramuscular injections[25] of serotype 2 adeno-associated virus (AAV2) results in gene delivery to MNs. In addition, MN gene delivery of insulin-like growth factor-1 (IGF-1) has proven to protect MNs both in vitro[45] and in vivo.[26] Identification of alternative protein targets for manipulation through gene transfer may provide a means of amplifying these neuroprotective effects.

Autoimmunity,[1] oxidative stress,[7,34] cytoskeletal abnormalities,[8] and excitotoxicity[37] have all been proposed as mechanisms triggering MN loss in ALS. A variety of evidence has emerged to support excitotoxicity in ALS patients and animal models of MN disease. First, MNs have demonstrated susceptibility to glutamate-induced death.[23] Second, abnormal glutamate metabolism has been noted in ALS.[36,42]

Abbreviations: AAV2, adeno-associated virus type 2; ALS, amyotrophic lateral sclerosis; Bcl-2, B-cell lymphoma 2; cDNA, complementary DNA; CMV, cytomegalovirus; CNS, central nervous system; DRG, dorsal root ganglia; EAAT2, excitatory amino acid transporter 2; E15, embryonic day 15; GFP, green fluorescent protein; HEK, human embryonic kidney; HEPES, *N*-(2-hydroxyethyl)piperazine-*N*′-(2-ethanesulfonic acid); HRP, horseradish peroxidase; IGF-1, insulin-like growth factor-1; IRES, internal ribosomal entry site; Islet-1, insulin 1 transcription factor; ITR(s), inverted terminal repeat sequences; MN, motor neuron; MOI, multiplicity of infection; NCAM, neural cell adhesion molecule; pA, polyadenylation; PAAv-IRES-hrGFP, plasmid adeno-associated virus internal ribosomal entry site Renilla green fluorescent protein; pAb, primary antibody; PAGE, polyacrylamide gel electrophoresis; PBS, phosphate-buffered saline; pDG, plasmid Dirk Grimm; PFA, paraformaldehyde; rAAV, recombinant adeno-associated virus; *SOD1*, superoxide dismutase gene 1; TUNEL, terminal deoxy-UTP nick-end labeling

Key words: amyotrophic lateral sclerosis; apoptosis; gene therapy; motor neuron disease; neuroprotection; primary motor neuron culture

Correspondence to: N. M. Boulis; e-mail: boulisn@ccf.org

Published online 22 August 2005 in Wiley InterScience (www.interscience.wiley.com). DOI 10.1002/mus.20418

Third, glutamate antagonists and increased glutamate buffering[2] have proven therapeutic in ALS. Most compelling, however, is the variety of data implicating abnormalities in glutamate transporters in ALS. *SOD1* mice have impaired high-affinity glutamate uptake.[9] Reduced levels of the excitatory amino acid transporter 2 (EAAT2) have been noted in the ventral horn of *SOD1* mutant rats.[22] Alterations in the molecular weight of the EAAT2 monomer have been noted in *SOD1* mice.[11] These observations have led us to adopt the assay using glutamate exposure to embryonic day 15 (E15) rat MNs as an in vitro model for ALS.[45]

Much evidence suggests that MN death in ALS occurs via an apoptotic mechanism. Apoptosis involves the activation of a specific intracellular cascade that culminates in DNA fragmentation and chromatin clumping. Proteases called caspases are a critical precursor to the cascade that culminates in DNA fragmentation. The caspase cascade is triggered by the release of mitochondrial contents including cytochrome *c*. Mitochondrial permeability is regulated in turn by the Bcl-2 family of proteins. Antiapoptotic members of the Bcl-2 family, including Bcl-$_X$L, prevent the formation of complexes that trigger the release of caspase-activating mitochondrial mediators. As an endogenous mechanism for cell removal, apoptosis triggers a minimal inflammatory response and therefore avoids collateral damage to functioning systems. This process is critical to the elimination of unnecessary cells during development, and damaged cells throughout life. However, apoptosis has been linked to a variety of neurodegenerative processes including ALS.[14] In *SOD1* mice, caspase-1 and caspase-3 are sequentially activated.[47] Caspase-9 activation, cytoplasmic cytochrome *c*, and mitochondrial Bax translocation, have also been documented in the *SOD1* mouse spinal cord.[20] We have previously demonstrated that glutamate exposure to cultured E15 MNs results in DNA fragmentation as measured by terminal deoxy-UTP nick-end labeling (TUNEL) and caspase-3 activation.[45] Expression of a mutant caspase-1 protein, capable of inhibiting apoptosis[15] as well as the intraventricular injection of small caspase inhibitors, improves the survival of *SOD1* mutant animals.[29] In addition, Bcl-2 overexpression delays caspase activation and increases MN survival in *SOD1* mice.[47] These data imply that antiapoptotic gene transfer targeted to MNs may provide a means to treat ALS.

Some success has been achieved with the transfer of antiapoptotic proteins in models of neurodegenerative disease. Azzouz et al.[2] demonstrated that intraspinal lumbar injections of a recombinant adeno-associated virus (rAAV) vector for the Bcl-2 gene improved neuromuscular function and MN survival. Kaspar et al.[24] showed that retrograde AAV delivery of the Bcl-$_X$L gene protected entorrhinal cortical neurons in a model of Alzheimer's disease. However, viral Bcl-$_X$L gene delivery has not previously been assessed as a means of MN protection.

In the present study, we constructed an AAV2 vector for the delivery of Bcl-$_X$L. In order to track gene expression, the gene for green fluorescent protein (GFP) was cloned in-frame upstream of the Bcl-$_X$L gene. Overexpression of vector-delivered Bcl-$_X$L was confirmed through western blots of protein obtained from cellular lysate. Gene expression by this vector plateaued 3 days after infection in both the SH-SY5Y neuroblastoma cell line and E15 MNs in vitro. After using TUNEL staining to establish the dose–response relationship of glutamate concentration to cell death, we evaluated the impact of the overexpression of Bcl-$_X$L on neuronal survival. AAV2-mediated overexpression of Bcl-$_X$L limited glutamate's ability to induce DNA fragmentation and reduce neuronal density in both SH-SY5Y and MN cultures. These findings suggest that AAV2-mediated MN Bcl-$_X$L delivery may provide an alternative approach to ALS therapy.

MATERIALS AND METHODS

Construction of AAV Bcl-$_X$L Vector. The human Bcl-$_X$L cDNA sequence was obtained from Manjunatha Bhat (Center for Anesthesiology Research, Cleveland Clinic Foundation) in the form of a fusion of the cDNA for GFP and Bcl-$_X$L, with the GFP sequence upstream of the Bcl-$_X$L sequence. The expression cassette contains the cytomegalovirus (CMV) promoter, GFP-Bcl-$_X$L fusion sequence, and polyadenylation (pA) sequence. The AAV2 shuttle vector, pAAV-IRES-hrGFP (Stratagene, La Jolla, California), containing a CMV promoter, multiple cloning sites, internal ribosomal entry site (IRES), GFP, and the SV40 pA signal, was used for the construction of a control vector (rAAV.GFP) that produces GFP. To create the experimental vector, pAAV-IRES-hrGFP was digested to remove the CMV, IRES, and the GFP sequence, exposing the AAV inverted terminal repeat (ITR) sequences. The GFP-Bcl-$_X$L expression cassette was then inserted between the ITRs, to produce pAAV.Bcl-$_X$L (Fig. 1A).

rAAV2 was produced by a cotransfection protocol developed by Grimm.[19] Plasmids pDG and pAAV.Bcl-$_X$L (experimental) or pAAV-IRES-hrGFP (control) were cotransfected into human embryonic kidney (HEK) 293 cells. The plasmid map of

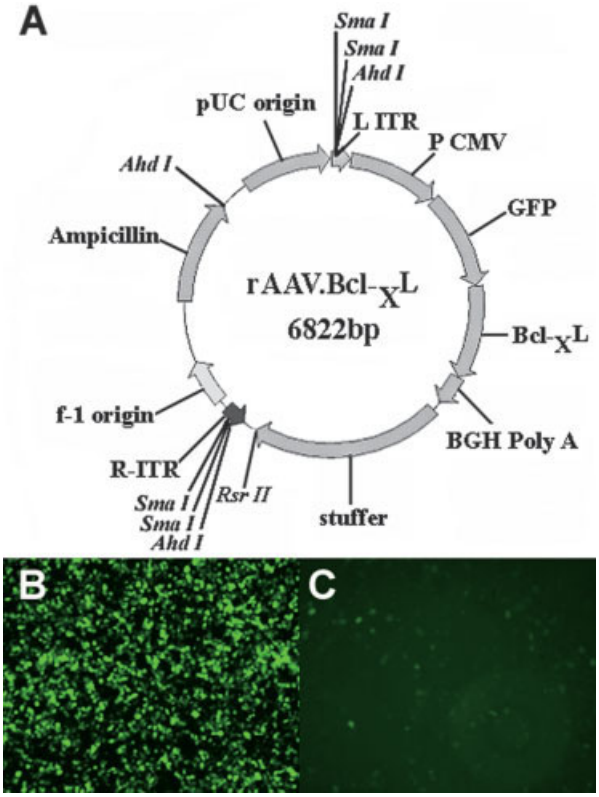

FIGURE 1. Production of rAAV.Bcl-$_X$L. **(A)** Map of plasmid rAAV.Bcl-$_X$L used for rAAV production. The fusion form of GFP and Bcl-$_X$L cDNA is under the control of the CMV promoter. The expression cassette is flanked by two adeno-associated virus ITRs. **(B)** GFP expression in HEK 293 cells infected with rAAV.Bcl-$_X$L. HEK 293 cells were coinfected with rAAV.Bcl-$_X$L (MOI 10) and a first generation of adenovirus (MOI 2) to boost gene expression. Forty-eight hours after infection, cells were observed for GFP expression under a fluorescent microscope. **(C)** HEK 293 cells infected with rAAV.IGF-1, which contains no GFP sequence, show minimal autofluorescence.

rAAV.Bcl-$_X$L is illustrated in Figure 1A. In order to boost the titer of rAAV, HEK 293 cells were coinfected with rAAV.Bcl-$_X$L at a multiplicity of infection (MOI) of 10 and with adenovirus at a MOI of 2. GFP was observed in cells 48 hours later under a fluorescent microscope (Leica, Bannockburn, Illinois) (Fig. 1B).

Cell Culture. SH-SY5Y cells were obtained from the American Tissue Culture Collection (ATCC, Manassas, Virginia) and grown to confluence in a 1:1 mixture of Eagle's minimum essential medium and Ham's F12 medium with 10% fetal bovine serum. Medium was renewed every 4 days and the cultures were monitored daily for signs of contamination.

Experiments were approved by the Cleveland Clinic Foundation animal care and use committee and adhered strictly to national requirements. For primary MN culture, spinal cords were obtained under sterile conditions from 15-day Sprague–Dawley rat embryos (Harlan, Indianapolis, Indiana) following an established protocol.[46] Dorsal root ganglia (DRG) and perineural membranes were removed and spinal cords were cut into approximately 2-mm sections and trypsinized. Cells were collected and centrifuged through a 6.8% metrizamide column (Sigma-Aldrich, St. Louis, Missouri) for 15 min at 2000 rpm. The upper layer of the gradient was collected and diluted in Leibowitz L-15 media (Invitrogen Life Technologies, Carlsbad, California). Pelleted cells were resuspended in complete growth medium made in Neurobasal medium (Invitrogen Life Technologies, Carlsbad, California) supplemented as previously described.[45] Cells were plated on poly-L-lysine–coated (Sigma-Aldrich) glass coverslips in multiwell tissue-culture plates (Fisher Scientific, Pittsburgh, Pennsylvania). Medium was renewed after 1 hour and neurite outgrowth was observed. To validate the motor neuron purification process, E15 mixed spinal cord cultures were plated using identical procedures, but eliminating the removal of DRG and metrizamide column separation steps.

Immunohistochemistry. Immunohistochemistry was performed with insulin 1 transcription factor (Islet-1), neural cell adhesion molecule (NCAM; University of Iowa, Iowa City, Iowa), and SMI-32 (Sternberger Monoclonals, Baltimore, Maryland) antibodies to evaluate MN homogeneity in the cultures. The SMI-32 antibody has been shown to be a specific indicator of nonphosphorylated neurofilaments in MNs.[3] NCAM (5A5) is an antibody to neurofilaments and selectively stains motor neurons within the embryonic spinal cord.[10] Islet-1 is an anti–transcription factor antibody, which has been shown to specifically label MNs.[13,44]

DNA fragmentation was evaluated with TUNEL staining, and apoptosis was evaluated using caspase-3 immunohistochemistry. Prior to staining, cells were fixed in 2% paraformaldehyde (PFA) for 10 min and rinsed in two washes of phosphate-buffered saline (PBS). TUNEL staining was performed with the Apoptag Plus peroxidase kit (Serologicals, Norcross, Georgia) and counterstained with hemotoxylin (Sigma-Aldrich). Caspase-3 immunohistochemistry was performed using anti-active caspase-3 primary antibody (pAb; Promega, Madison, Wisconsin). The secondary antibody was Texas Red fluorescence conjugated (Jackson ImmunoResearch Labs, West Grove, Pennsylvania).

Glutamate-Induced Apoptosis. Glutamate-induced cytotoxicity was assessed in both the SH-SY5Y neuroblastoma cell line and in primary MNs. Cells were exposed to glutamate at concentrations of 10, 50, or 100 μM or PBS for 1 hour. Medium was changed, and cells were allowed to remain in culture for 24 hours prior to TUNEL staining. Quantification of TUNEL-positive cells was done with random counts from three areas in each of three different wells using light microscopy (Leica, Buffalo, New York). The percentages of TUNEL-positive cells in each condition were quantified and statistically analyzed.

To measure cell density changes, three random areas in each well were photographed using an inverted Leica DM IL light microscope and the Q Imaging Micropublisher System (version 3.3) with Q Imaging Capture Suite software (Q Imaging, Burnaby, BC, Canada) immediately before and 24 hours after glutamate insult. The ratio of the mean number of cells following glutamate exposure to the number of cells prior to glutamate exposure was quantified and expressed as a mean percentage ($\pm$SEM) of remaining cell density (N = 3/condition).

Timeline of Gene Expression. For all viral inoculations, the rAAV.Bcl-$_X$L and the rAAV.GFP were suspended in 10 mM HEPES and 150 mM NaCl buffer at pH 7.6. Medium was removed and this solution was added to the cells and rocked gently for 60 seconds every 10 min, three consecutive times, to ensure equal distribution of the viral suspension over the cells.

To determine the time-course of Bcl-$_X$L gene expression, SH-SY5Y cells were exposed to either rAAV.Bcl-$_X$L at 20 MOI or PBS. Similarly, MNs were exposed to rAAV.Bcl-$_X$L at 20 MOI and at 100 MOI or PBS. Cells were fixed in 2% PFA and observed under fluorescent microscopy after 24 and 48 hours and then every other day for up to 14 days. Cells positive for GFP expression (Fig. 2E and G) were counted in three random areas in each of three wells, and the mean percentage $\pm$ SEM of GFP-positive cells was calculated. As a separate negative control for autofluorescence, SH-SY5Y cells and MNs were infected with rAAV.IGF-I and examined at 10 days.

Western Blot Analysis of Bcl-$_X$L Gene Expression. Identification and levels of expression of viral Bcl-$_X$L protein were analyzed using western blotting techniques. Protein was extracted from SHSY-5Y cells following exposure to 20 MOI rAAV.Bcl-$_X$L for 24 hours and 2, 4, 8, and 12 days and from SHSY-5Y cells following exposure to 20 MOI rAAV.GFP after 4 days. Protein concentration was estimated according to the Bradford assay method. Samples were loaded using polyacrylamide gel electrophoresis (PAGE) and western blots were performed using an antibody to human Bcl-$_X$L (Santa Cruz Biotechnology, Santa Cruz, California). The secondary antibody was horseradish peroxidase (HRP) conjugated. The blot was stripped and reprobed using an antibody to β-actin (Sigma-Aldrich) to confirm equal protein loading in each lane.

Gene-Based Neuroprotection in Models of MN Disease In Vitro. Seven days after exposure to rAAV.Bcl-$_X$L (20 MOI), rAAV.GFP (20 MOI), or PBS, SH-SY5Y cells were exposed to 10 μM glutamate for 1 hour. In contrast, MNs were exposed to 100 μM glutamate for 1 hour, 4 days after exposure to either PBS, rAAV.Bcl-$_X$L (100 MOI), or rAAV.GFP (100 MOI). Cells were allowed to recover in fresh media for 24 hours and then fixed and TUNEL stained as described earlier. Quantification of total cells and cells positive for TUNEL staining was done at 400$\times$ magnification in three random fields per well in every condition. The mean cell density and percentage of cells positive for TUNEL staining were calculated in each group and assessed using analysis of variance (ANOVA).

Statistical Analysis. Statistical analyses of data were performed, and mean $\pm$ SEM are reported. Significance levels as assessed by ANOVA and either Tukey's or Dunn's tests are reported as $P < 0.05$, $P < 0.01$, or $P < 0.001$. Statistical analysis was performed with SigmaStat software (Windows version 2.0, 1992–1995; SigmaStat, Chicago, Illinois).

RESULTS

AAV2 vectors containing the GFP-Bcl-$_X$L protein or GFP alone were constructed by cotransfection with pDG as previously described (Fig. 1A).[18] Figure 1B confirms the production of the GFP-Bcl-$_X$L transgene product (Fig. 1B) in HEK 293 cells exposed to an rAAV (MOI 10) with helper adenovirus (MOI 2). Minimal autofluorescence is detected in HEK 293 cells infected at the same titer with rAAV.IGF-1, which contains no GFP sequence.

Islet-1 (Fig. 2A and B), NCAM, and SMI 32 immunohistochemistry confirmed that 94% of the cells in enriched E15 spinal cord cultures were MNs. Mixed E15 spinal cord cultures were stained for Islet-1 to validate the staining technique, illustrating the increase in MNs provided by metrizamide puri-

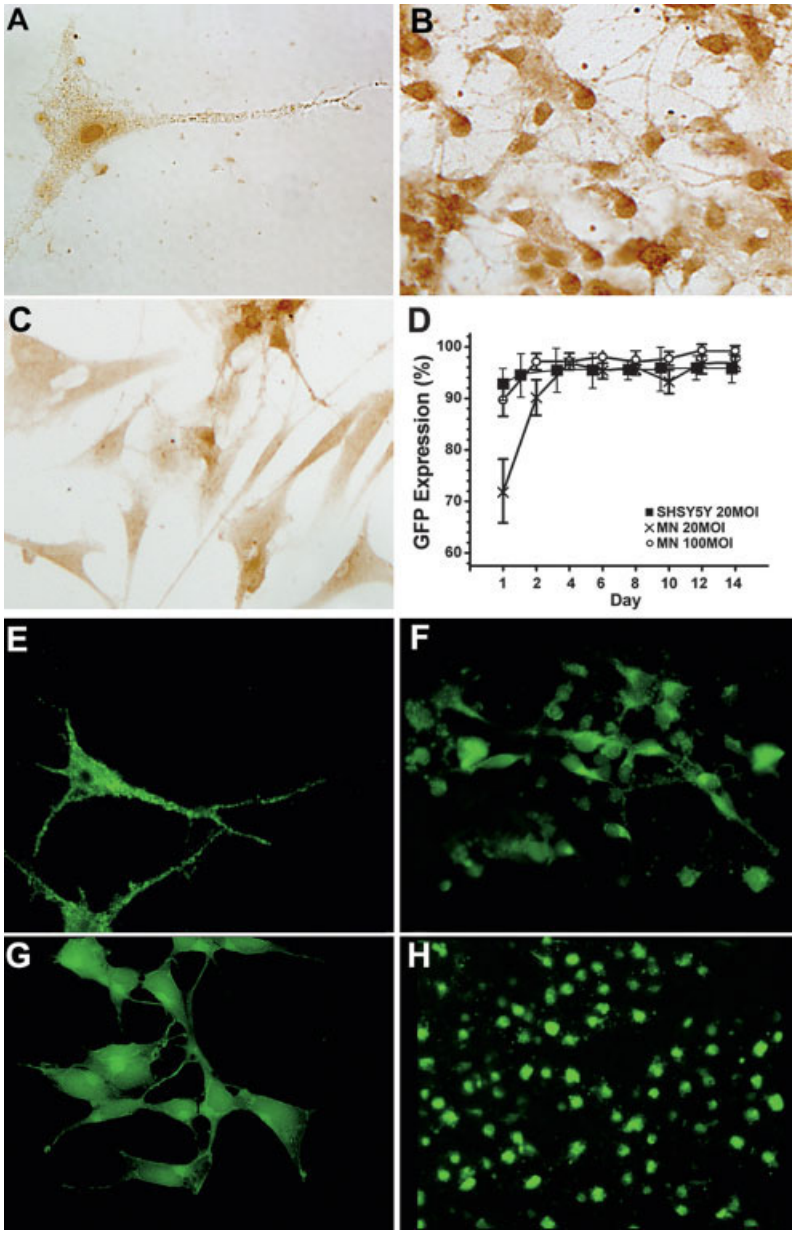

FIGURE 2. Motor neuron homogeneity and GFP expression following viral infection in vitro. Immunohistochemistry performed with various antibodies including Islet-1 **(A, B)**, NCAM, and SMI 32 (images not shown) confirmed MN enrichment (94%) in vitro. Mixed E15 spinal cord cultures illustrate the enrichment of MNs achieved through selective dissection and metrizamide purification **(C)**. Green fluorescence confirms the presence of viral transgene production in rAAV.Bcl-$_X$L–infected (20 MOI) SH-SY5Y cells **(E, F)** and E15 MNs **(G, H)**. Time-course of gene expression established in primary MNs following infection with rAAV.Bcl-$_X$L at 20 and 100 MOI and SH-SY5Y cells at 20 MOI **(D)**. Viral transgene expression is observed in approximately 90% of motor neurons 24 hours after infection at 100 MOI (denoted in graph by the ○ symbol). A similar pattern of transgene expression is observed in SH-SY5Y cells at 20 MOI (denoted in graph by the ■ symbol).

fication (Fig. 2C). Both SH-SY5Y neuroblastoma cells and the enriched MN cultures were infected with rAAV.Bcl-$_X$L. Consistent GFP expression was evident in both SH-SY5Y cells (Fig. 2E and F) and MNs (Fig. 2G and H). The percentage of neurons expressing the fusion protein was recorded as a function of time for SH-SY5Y cells infected with 20 MOI and primary MNs infected at both 20 and 100 MOI of rAAV.Bcl-$_X$L (Fig. 2D). This experiment helped to establish the appropriate titer and timing for neural protection experiments. Because SH-SY5Y cells proliferate continually, whereas E-15 cultured MNs deteriorate within 2–3 weeks, expression was tracked for 14 days. Over 90% of SH-SY5Y cells showed trans-

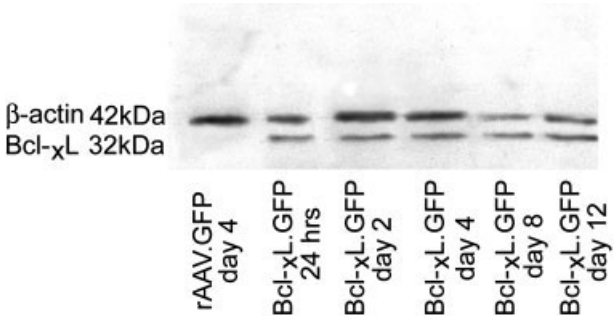

FIGURE 3. Adeno-associated virus vector–mediated overexpression of Bcl-$_X$L. SH-SY5Y neuroblastoma cells were exposed to rAAV.Bcl-$_X$L or rAAV.GFP for 24 hours. Bcl-$_X$L expression (32 kDa) was confirmed by anti–Bcl-$_X$L western blots of cell lysates made at various intervals following infection. Blots were stripped and reprobed with anti–β-actin to confirm uniform protein loading (42 kDa). As predicted by the GFP expression time-course, transgene expression varied little after 24 hours. Bcl-$_X$L expression was not detected in SH-SY5Y cells exposed to the control vector, rAAV.GFP.

gene expression 24 hours after infection, whereas primary MNs required 48 hours to reach a comparable level at 20 MOI. Two-way ANOVA revealed that GFP expression varied as a function of time ($N = 36$; $P < 0.018$). Transgene expression appeared to plateau by day 4 in primary MNs at both titers. Overexpression of the viral Bcl-$_X$L protein was further confirmed in the SH-SY5Y cell line using western blotting techniques (Fig. 3). Compared to the control rAAV.GFP condition 4 days after infection, the rAAV.Bcl-$_X$L–infected cells demonstrated a positive result, appearing as a band at a molecular weight of 32 kDa. An internal control for β-actin appeared as a positive band at 42 kDa and remained at a consistent level throughout (Fig. 3).

To complete the in vitro model for MN disease, 24 hours after exposure to a variety of L-glutamic acid concentrations TUNEL staining was performed on both the SH-SY5Y cell line (Fig. 4A) and primary MN cultures (Fig. 4B). ANOVA revealed a significant glutamate concentration effect in both SH-SY5Y cells ($N = 36$; $P < 0.001$) and E15 MNs ($N = 36$; $P < 0.001$). Similar results were confirmed via analysis of caspase-3 positivity.

Initial efforts to demonstrate neuroprotection by rAAV.Bcl-$_X$L were focused on the SH-SY5Y model. Because rAAV expression in vivo peaks after 1 week and SH-SY5Y survival in culture remains robust, cultures were infected at 20 MOI at 7 days prior to glutamate insult. Consistent with the percent infection curve depicted in Figure 2D, 94% of SH-SY5Y cells were fluorescent, suggesting infection with either control or experimental vector. TUNEL staining and cell density were observed in SH-SY5Y cells, 24 hours after a 10-μM glutamate insult (Fig. 5C). Under control conditions, 10 μM glutamate caused 20 ± 3% of cells to develop positive TUNEL staining and a reduction of cell density to 60 ± 4%. Figure 5A demonstrates that 4.5% of neuronal cells in cultures infected with rAAV.Bcl-$_X$L stained positive for TUNEL in comparison to 26.5% and 20% in the control rAAV.GFP and PBS conditions, respectively ($N = 27$; $P < 0.001$). Loss of cellular adhesion accompanying the apoptotic process was reflected by a reduction in cell density in SH-SY5Y cells exposed to glutamate insult (Fig. 5C vs D). Cells retained 96% of their pre-glutamate density in the rAAV.Bcl-$_X$L-GFP condition, whereas only 58% and 62% of cells remained in the rAAV.GFP and PBS conditions, respectively (Fig. 5B; $N = 27$; $P < 0.001$). In addition to increased density, cells in the rAAV.Bcl-$_X$L condition appeared morphologically healthier, maintaining intact membranes, cellular compartment integrity, and proper size and shape (Fig. 5D) compared to cells in control conditions (Fig. 5C). TUNEL staining has previously been documented in cells undergoing necrotic as opposed to apoptotic cell death. To confirm that TUNEL and density measurements reflect apoptotic cell death, SH-SY5Y cells were stained for caspase-3 activation using the same glutamate toxicity and vector-based protection protocol. Figure 6 illustrates caspase-3 staining after glutamate exposure in cells exposed to vehicle (Fig. 6A) as compared to cells exposed to rAAV.Bcl-$_X$L (Fig. 6B). In addition to the reduction in overall caspase-3 staining, cells expressing the fusion protein transgene (green) had notably less caspase-3 positivity.

Based on the more rapid gene expression in MNs infected at 100 MOI, neuroprotection experiments were conducted at this titer. MNs were exposed to 100 μM glutamate for 1 hour, 4 days after infection with rAAV2. We found that 92% of MNs were in-

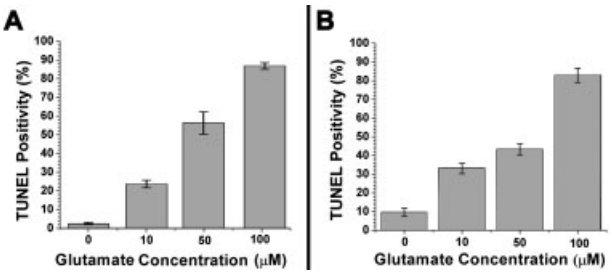

FIGURE 4. Glutamate-induced TUNEL staining dose–response curves. **(A)** SH-SY5Y cells and **(B)** primary MNs were exposed to PBS or glutamate at 10, 50, and 100 μM for 1 hour. DNA fragmentation was measured with TUNEL staining 24 hours after glutamate exposure.

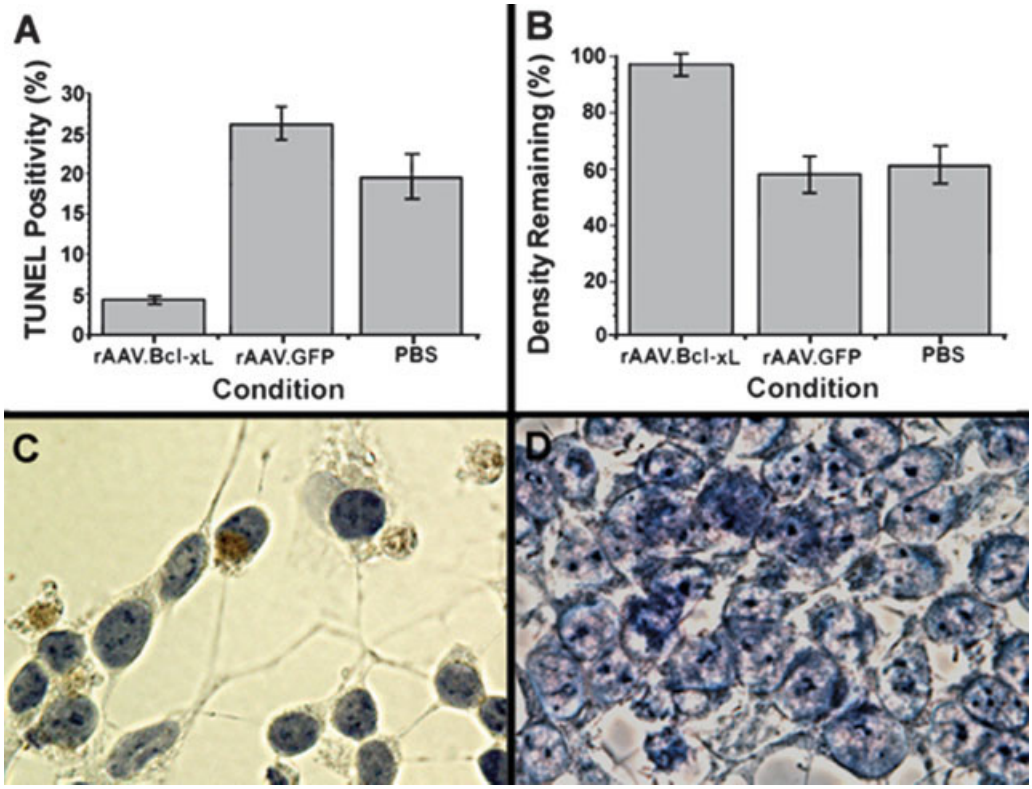

FIGURE 5. SH-SY5Y neuronal cell line protection against glutamate-induced excitotoxicity. **(A)** Overexpression of Bcl-$_X$L achieved through the delivery of the rAAV.Bcl-$_X$L vector in SH-SY5Y cells decreased TUNEL staining from 26.5% in the control rAAV.GFP condition to 4.5% in the Bcl-$_X$L condition, following glutamate insult ($N = 27$, $P < 0.001$). **(B)** The Bcl-$_X$L condition retained 96% of pre–glutamate-induced cell density compared to 58% in the GFP control condition ($N = 27$; $P < 0.001$). **(C)** TUNEL positivity indicated by brown staining and decreased cellular density were observed to a greater degree in control conditions. **(D)** TUNEL staining is reduced and density is preserved in SH-SY5Y cells pretreated with rAAV.Bcl-$_X$L.

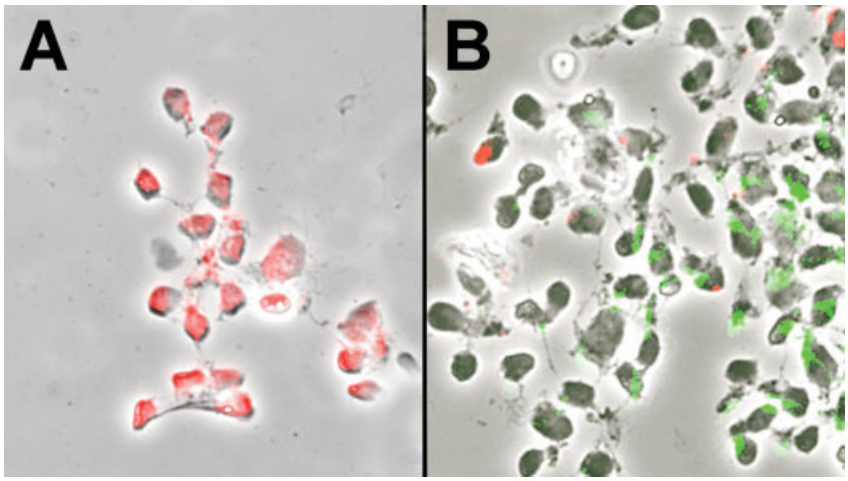

FIGURE 6. Glutamate exposure activates caspase-3 in SH-SY5Y cells. **(A)** Exposure of control SHSY-5Y cells in the PBS condition to 10 μM glutamate for 1 hour induced decreased cellular density and caspase-3 activation as detected by immunohistochemistry (Texas red). **(B)** In the rAAV.Bcl-$_X$L condition, the lack of colocalization of vector transgene (green fluorescence) with caspase-3 positivity (red fluorescence) reinforced the protective effects of rAAV.Bcl-$_X$L against apoptosis.

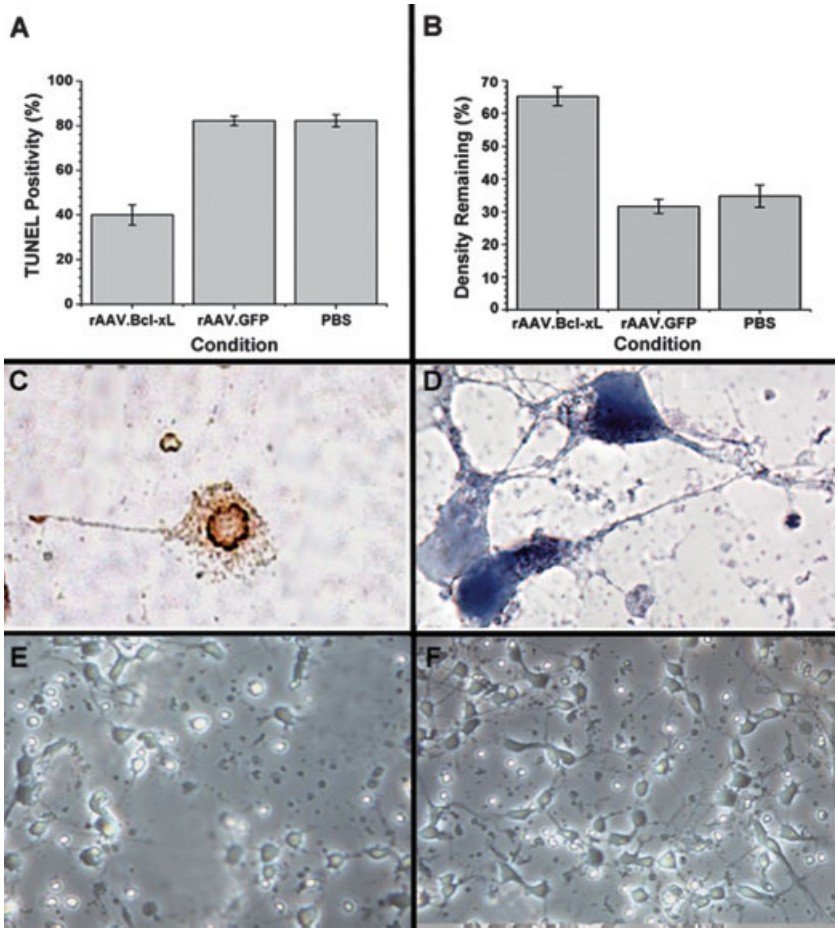

FIGURE 7. MN protection against glutamate-induced excitotoxicity. **(A)** Overexpression of Bcl-$_X$L achieved through the delivery of the rAAV.Bcl-$_X$L vector in primary cultured motor neurons reduced TUNEL staining from 82.3% in the control rAAV.GFP condition to 39.9% in the rAAV.Bcl-$_X$L condition ($N = 27$, $P < 0.001$). **(B)** The Bcl-$_X$L condition retained 66% of pre–glutamate-induced cell density as compared to 32% in the rAAV.GFP condition ($N = 27$; $P < 0.01$). **(C)** TUNEL-positive cells indicated by brown staining, in addition to decreased cellular density, were observed in the control rAAV.GFP condition following glutamate insult. **(D)** TUNEL-negative MNs with preserved cell density following glutamate exposure in the rAAV.Bcl-$_X$L condition. MNs were counterstained with hematoxylin in order to visualize otherwise transparent cellular membranes.

fected based on fluorescence. An earlier timepoint was utilized for the MN assay because these cells have a limited longevity in culture. Figure 7A reveals that Bcl-$_X$L overexpression in primary cultured motor neurons reduced TUNEL staining from 82.3% and 80% in the control rAAV.GFP and PBS conditions to 39.9% in the rAAV.Bcl-$_X$L condition ($N = 27$; $P < 0.001$). Pairwise comparison (Tukey's test) between the mean of the rAAV.Bcl-$_X$L group and either the rAAV.GFP or PBS groups reached significance, but was not significant between the rAAV.GFP and PBS groups. This finding suggests that rAAV2 induces no MN death and that the protective effects are transgene-specific. Like SH-SY5Y cells, MNs lose adhesion capability during apoptosis. The Bcl-$_X$L condition retained 66% of pre-glutamate MN cell density as compared to 32% and 35.7% of cells remaining in the rAAV.GFP and PBS conditions, respectively (Fig. 7B; $N = 27$; $P < 0.01$). The differences in the mean values between the Bcl-$_X$L condition groups and control groups indicated significant remaining density in the Bcl-$_X$L condition ($P < 0.01$). Importantly, comparison of the various conditions revealed no difference in the MN density prior to glutamate exposure. Across all conditions, the number of MNs counted in three frames was 99.630 ± 1.794 (mean ± SEM).

DISCUSSION

The present study replicates our previous finding that glutamate triggers neuronal death culminating in DNA fragmentation in both a neuronal cell line (SH-SY5Y) and primary neuronal culture (E15

MNs). This toxicity obeys predictable dose–response characteristics in both preparations. Similarly, close to 100% of neurons show reporter gene expression within 3 days of infection. Finally, Bcl-$_X$L gene expression significantly reduces cell death induced via glutamate toxicity as measured by reduced TUNEL and cell density in both SH-SY5Y cells and primary motor neurons.

The impact of Bcl-$_X$L expression on glutamate-induced cell death further supports the conclusion that this is an apoptotic process. Although a variety of assays exist for analysis of apoptosis, TUNEL staining was the primary assay of apoptosis in the current study. TUNEL staining is not entirely specific for apoptosis, however, sometimes detecting necrotic cell death.[17,41] Apoptosis is reflected by morphological changes in the cell, including cellular membrane blebbing, cellular shrinking, and chromatin clumping.[27,31] Morphological alterations of this type have been observed in the present model system, but have not been rigorously characterized. We have previously reported immunohistochemical evidence of caspase-3 activation colocalized with TUNEL staining in E15 MNs following exposure to glutamate.[45] In the present experiment, caspase-3 staining was performed on SH-SY5Ys 24 hours after glutamate exposure and 7 days after rAAV.Bcl-$_X$L or vehicle exposure. Caspase-3 activation is observed to parallel the observed protection documented with TUNEL and cell density. Because Bcl-$_X$L expression should exert protective effects against apoptotic death but not necrotic death, the current data provide further evidence that glutamate excitotoxicity induces apoptosis in the SH-SY5Y and E15 MN models.

Neuronal gene expression by rAAV2 vectors tends to occur more slowly than the expression induced by a variety of early generation vectors. rAAV-induced gene expression in the brain begins within the first week of injection.[40,43] Despite the apparent in vivo delay in rAAV2 gene expression, AAV2 particles transit from the extracellular space to the nuclei of brain neurons within 30 minutes.[4] Consistent with this observation, rAAV2 gene expression in vitro occurs within 48 hours.[30] Less is known about the timeline of rAAV2 gene expression in primary neuronal culture. The present experiment reflects this previously documented timeline for expression in vitro. The health of E15 MNs in culture deteriorates over time. In order to optimize gene expression and the pre–glutamate-exposed health of the MNs, we assayed the impact of glutamate 4 days after rAAV infection. The more robust nature of the SH-SY5Y model allowed for the glutamate assay to be performed 7 days following infection.

To our knowledge, Bcl-$_X$L has not been previously documented to protect motor neurons. However, this transgene has been effectively applied in models of neurodegenerative disease elsewhere in the central nervous system (CNS). Matsuoka et al.[32] demonstrated enhanced survival of E16 cortical neurons in vitro following adenovirus vector–mediated Bcl-$_X$L expression. Transection of the perforant pathway causes axotomy-induced cell death in the entorhinal cortex and has been applied as a model of the neuronal death observed in this region in Alzheimer's disease. Kaspar et al.[24] demonstrated that retrograde AAV2-mediated Bcl-$_X$L expression could prevent entorhinal death in this model. Sciatic transection causes apoptosis of MNs projecting into the nerve. In parallel to neuronal degeneration, MNs show evidence of BAX upregulation, whereas Bcl-2 and Bcl-$_X$L remain present in moderate to low levels.[16] Bcl-2 and Bcl-$_X$L prevent proapoptotic BAX dimerization. Thus, the axotomy model suggests that reducing the BAX:Bcl-2/Bcl-$_X$L ratio might prevent MN apoptosis. Consistent with this hypothesis, Azzouz et al.[2] demonstrated that AAV2-mediated Bcl-2 expression in spinal cord protects MNs from death in the *SOD1* mutant mouse model. Similarly, *IGF-1* gene expression, which inhibits apoptosis, prevents MN apoptosis in vitro[45] and in the *SOD1* mouse model.[26] These data support application of Bcl-$_X$L MN gene transfer as a therapeutic strategy for ALS.

Despite the fact that apoptosis may form the final common pathway of cell death in these disorders, saving neurons by interrupting the apoptotic cascade may not be sufficient to relieve the associated symptoms of neurodegenerative disease. Some evidence suggests that neurons may have already suffered irreversible damage to their functional machinery prior to the initiation of apoptosis.[12] This evidence centers on the observation that antiapoptotic approaches often prevent neuronal death without salvaging neural function. Yamada et al.[49] noted that herpes simplex virus–mediated Bcl-2 gene transfer to MNs prevented axotomy-induced death, but failed to restore a cholinergic phenotype to the cells. Similarly, in the progressive motor neuronopathy model of ALS, Bcl-2 overexpression prevented MN death but not axonal degeneration.[39] In models of cerebral ischemia, Bcl-2 overexpression prevented neuronal death in the hippocampus, but did not spare the ability of these neurons to maintain the posttetanic potentiation form of synaptic plasticity. Similarly, caspase inhibitors preserved neurons in the hippocampus following ischemia, but did not preserve long-term potentiation.[16] Herpes simplex virus-1–mediated Bcl-2 delivery was able to reduce

the size of kianic acid lesions (excitotoxicity) in the hippocampus, but did not preserve hippocampal function as measured by spatial memory.[33] In contrast, however, overexpression of Bcl-2 in *SOD1* mutant mice reduced muscle denervation and prolonged survival.[28] Similarly, as previously discussed, intracerebroventricular caspase inhibitors[29] maintain strength and prolong survival in *SOD1* animals. Thus, at least in the *SOD1* model of ALS, preventing MN loss by interrupting the apoptotic cascade late in the process has the potential to provide a functional therapeutic outcome.

The authors are grateful to Eva Feldman, Andrea Vincent, Bret Mobley, and Carrie Backus at the University of Michigan for their support with primary motor neuron culture. In addition, we are indebted to Manjunatha Bhat in the Center for Anesthesiology Research at the Cleveland Clinic Foundation for providing the cDNA for the GFP-Bcl-$_X$L fusion protein. This work was supported by grants from the NIH, the ALS Association, Hope for ALS, and the Christopher Reeve Paralysis Foundation.

REFERENCES

1. Appel SH, Smith RG, Engelhardt JI, Stefani E. Evidence for autoimmunity in amyotrophic lateral sclerosis. J Neurol Sci 1994;124:14–19.
2. Azzouz M, Hottinger A, Paterna JC, Zurn AD, Aebischer P, Bueler H. Increased motoneuron survival and improved neuromuscular function in transgenic ALS mice after intraspinal injection of an adeno-associated virus encoding Bcl-2. Hum Mol Genet 2000;9:803–811.
3. Bar-Peled O, Knudson M, Korsmeyer S, Rothstein J. Motor neuron degeneration is attenuated in bax-deficient neurons in vitro. J Neurosci Res 1999;320:291–303.
4. Bartlett JS, Samulski RJ, McCown TJ. Selective and rapid uptake of adeno-associated virus type 2 in brain. Hum Gene Ther 1998;9:1181–1186.
5. Borasio G, Miller R. Clinical characteristics and management of ALS. Semin Neurol 2001;21:155–166.
6. Boulis NM, Noordmans AJ, Song DK, Imperiale MJ, Rubin A, Leone P, et al. Adeno-associated viral vector gene expression in the adult rat spinal cord following remote vector delivery. Neurobiol Dis 2003;14:535–541.
7. Bowling A, Barkowski E, McKenna-Yasek D, Sapp P, Horvitz H, Beal M, et al. Superoxide dismutase concentration and activity in familial amyotrophic lateral sclerosis. J Neurochem 1995;64:2366–2369.
8. Bruijn L, Cleveland D. Mechanisms of selective motor neuron death in ALS: insights from transgenic mouse models of motor neuron disease. Neuropathol Appl Neurobiol 1996;22: 373–387.
9. Canton T, Pratt J, Stutzmann J, Imperato A, Boireau A. Glutamate uptake is decreased tardively in the spinal cord of FALS mice. Neuroreport 1998;9:775–778.
10. Chen E, Chiu A. Early stages in the development of spinal motor neurons. J Comp Neurol 1992;320:291–303.
11. Deitch J, Alexander G, Del Valle L, Heiman-Patterson T. GLT-1 glutamate transporter levels are unchanged in mice expressing G93A human mutant *SOD1*. J Neurol Sci 2002;193: 117–126.
12. Dumas T, Sapolsky R. Gene therapy against neurological insults: sparing neurons versus sparing function. Trends Neurosci 2001;24:695–700.
13. Ericson C, Wictorin K, Lundberg C. Ex vivo and in vitro studies of transgene expression in rat astrocytes transduced with lentiviral vectors. Exp Neurol 2002;173:22–30.
14. Friedlander R. Apoptosis and caspases in neurodegenerative diseases. N Engl J Med 2003;348:1365–1375.
15. Friedlander R, Brown R Jr, Gagliardini V, Wang J, Yuan J. Inhibition of ICE slows ALS in mice. Nature 1997;388:31.
16. Gillardon F, Kiprianova I, Sandkuhler J, Hossmann K, Spranger M. Inhibition of caspases prevents cell death of hippocampal CA1 neurons, but not impairment of hippocampal long-term potentiation following global ischemia. Neuroscience 1999;93:1219–1222.
17. Grasl-Kraupp B, Ruttkay-Nedecky B, Koudelka H, Bukowska K, Bursch W, Schulte-Hermann R. In situ detection of fragmented DNA (TUNEL assay) fails to discriminate among apoptosis, necrosis, and autolytic cell death: a cautionary note. Hepatology 1995;21:1465–1468.
18. Grimm D, Kern A, Rittner K, Kleinschmidt J. Novel tools for production and purification of recombinant adenoassociated virus vectors. Hum Gene Ther 1998;9:2745–2760.
19. Grimm D, Kleinschmidt J. Progress in adeno-associated virus type 2 vector production: promises and prospects for clinical use. Hum Gene Ther 1999;10:2445–2450.
20. Guegan C, Vila M, Rosoklija G, Hays AP, Przedborski S. Recruitment of the mitochondrial-dependent apoptotic pathway in amyotrophic lateral aclerosis. J Neurosci 2001;21:6569–6576.
21. Gurney ME, Pu H, Chiu AY, Dal Canto MC, Polchow CY, Alexander DD, et al. Motor neuron degeneration in mice that express a human CuZn superoxide dismutase mutation. Science 1994;264:1772–1775.
22. Howland DS, Liu J, She Y, Goad B, Maragakis NJ, Kim B, et al. Focal loss of the glutamate transporter EAAT2 in a transgenic rat model of *SOD1* mutant-mediated amyotrophic lateral sclerosis (ALS). Proc Natl Acad Sci USA 2002;99:1604–1609.
23. Ikonomidou C, Qin Y, Labruyere J, Olney J. Motor neuron degeneration induced by excitotoxin agonists has features in common with those seen in the *SOD-1* transgenic mouse model of amyotrophic lateral sclerosis. J Neuropathol Exp Neurol 1996;55:211–224.
24. Kaspar B, Schaffer D, Erickson D, Hinh L, Peterson D, Gage F. Neuroprotection in an Alzheimer's disease model by retrograde transport of an AAV expressing an anti-apoptotic gene. Mol Ther 2001;3(suppl):S119.
25. Kaspar BK, Erickson D, Schaffer D, Hinh L, Gage FH, Peterson DA. Targeted retrograde gene delivery for neuronal protection. Mol Ther 2002;5:50–56.
26. Kaspar BK, Llado J, Sherkat N, Rothstein JD, Gage FH. Retrograde viral delivery of IGF-1 prolongs survival in a mouse ALS model. Science 2003;301:839–842.
27. Kerr J, Wyllie A, Currie A. Apoptosis: a basic biological phenomenon with wide ranging implications in tissue kinetics. Br J Cancer 1972;26:239–257.
28. Kostic V, Jackson-Lewis V, de Bilbao F, Dubois-Dauphin M, Przedborski S. Bcl-2: prolonging life in a transgenic mouse model of familial amyotrophic lateral sclerosis. Science 1997; 277:599–562.
29. Li M, Ona VO, Guegan C, Chen M, Jackson-Lewis V, Andrews LJ, et al. Functional role of caspase-1 and caspase-3 in an ALS transgenic mouse model. Science 2000;288:335–339.
30. Luo J, Murphy L. Differential expression of insulin-like growth factor-I and insulin-like growth factor binding protein-I in the diabetic rat. Mol Cell Biol 1991;103:41–50.
31. Majno G, Joris I. Apoptosis, oncosis, and necrosis: an overview of cell death. Am J Pathol 1995;146:3–15.
32. Matsuoka N, Yukawa H, Ishii K, Hamada H, Akimoto M, Hashimoto N, et al. Adenovirus-mediated gene transfer of Bcl-xL prevents cell death in primary neuronal culture of the rat. Neurosci Lett 1999;270:177–180.
33. McLaughlin J, Roozendaal B, Dumas T, Gupta A, Ajilore O, Ho D, et al. Sparing of neuronal function postseizure with gene therapy. Proc Natl Acad Sci 2000;97:12804–12809.

34. Mitsumoto H, Ikeda K, Klinkosz B, Cedarbaum J, Wong V, Lindsay R. Arrest of motor neuron disease in wobbler mice co-treated with CNTF and BDNF. Science 1994;265:1107–1110.
35. Rosen DR, Siddique T, Patterson D, Figlewicz DA, Sapp P, Hentati A, et al. Mutations in Cu/Zn superoxide dismutase gene are associated with familial amyotrophic lateral sclerosis. Nature 1993;362:59–62.
36. Rothstein J, Tsai G, Kuncl R, Clawson L, Cornblath D, Drachman D, et al. Abnormal excitatory amino acid metabolism in amyotrophic lateral sclerosis. Ann Neurol 1990;28:18–25.
37. Rothstein J, Van Kammen M, Levey A, Martin L, Kuncl R. Selective loss of glial glutamate transporter GLT-1 in amyotrophic lateral sclerosis. Ann Neurol 1995;38:73–84.
38. Rowland L. How amyotrophic lateral sclerosis got its name: the clinical–pathologic genius of Jean-Martin Charcot. Arch Neurol 2001;58:512–515.
39. Sagot Y, Dubois-Dauphin M, Tan S, de Bilbao F, Aebischer P, Martinou J, et al. Bcl-2 overexpression prevents motoneuron cell body loss but not axonal degeneration in a mouse model of a neurodegenerative disease. J Neurosci 1995;15:7727–7733.
40. Sanchez-Pernaute R, Harvey-White J, Cunningham J, Bankiewicz K. Functional effect of adeno-associated virus mediated gene transfer of aromatic L-amino acid decarboxylase into the striatum of 6-OHDA-lesioned rats. Mol Ther 2001;4:324–330.
41. Schaper J, Elasser A, Kostin S. The role of cell death in heart failure. Circ Res 1999;85:867–869.
42. Spreux-Varoquaux O, Benisimon G, Lacomblez L, Salachas F, Pradat P, LeForestier N, et al. Glutamate levels in cerebrospinal fluid in amyotrophic lateral sclerosis: a reappraisal using a new HPLC method with coulometric detection in a large cohort of patients. J Neurol Sci 2002;193:73–78.
43. Tenenbaum L, Jurysta F, Stathopoulos A, Puschban Z, Melas C, Hermens W. Tropism of AAV-2 vectors for neurons of the globus pallidus. Neuroreport 2000;11:2277–2283.
44. Tsuchida T, Ensini M, Morton S, Baldassare M, Edlund T, Jessell T, et al. Topographic organization of embryonic motor neurons defined by expression of LIM homeobox genes. Cell 1994;79:957–970.
45. Vincent A, Boulis N, Jung V, Song D, Imperiale M, Feldman E. AAVCMV.IGF-I.IRES.GFP based neuroprotection in an in vitro model of amyotrophic lateral sclerosis. Mol Ther 2002;5(suppl):S96.
46. Vincent A, Feldman E. Control of cell survival by IGF signaling pathways. Growth Horm IGF Res 2002;12:193–197.
47. Vukosavic S, Stefanis L, Jackson-Lewis V, Guegan C, Romero N, Chen C, et al. Delaying caspase activation by Bcl-2: a clue to disease retardation in a transgenic mouse model of amyotrophic lateral sclerosis. J Neurosci 2000;20:9119–9125.
48. Wong P, Borchelt D. Motor neuron disease caused by mutations in superoxide dismutase 1. Curr Opin Neurol 1995;8:294–301.
49. Yamada M, Tanabe K, Wada K, Shimoke K, Ishidawa Y, Ikeuchi T, et al. Differences in survival-promoting effects and intracellular signaling properties of BDNF and IGF-1 in cultured cerebral cortical neurons. J Neurochem 2001;78:940–951.